DOI: 10.1002/cphc.200800663

Differential Sensing of Serine and Tyrosine with Aligned CdS Nanowire Arrays Based on pH-Dependent Photoluminescence Behavior

Yi-Feng Lin,[a] Yung-Jung Hsu,[b] Wei-Yun Cheng,[a] and Shih-Yuan Lu*[a]

The differential sensing of tyrosine and serine is achieved with well-aligned CdS nanowire arrays by exploring the pH-dependent photoluminescence behavior of the nanowire arrays toward exposure to the two amino acid solutions. The contrasting trend in photoluminescence (PL) intensity with respect to variations in analyte concentration observed at pH 11 served as the check point for the present differential sensing. The application format of the nanowire array is better suited for further sensing device assembly than that of nanocrystal suspensions.

1. Introduction

Since the pioneering work of Bruchez, Jr. et al.[1] and Chen and Nie[2] on biological detection by fluorescent nanocrystals, extensive developments have been made to demonstrate the excellent sensing ability of semiconductor nanocrystal suspensions toward a wide range of biosubstances, including paraoxon,[3] spironolactone,[4] protease,[5] urea[6] and amino acids[7] through the quenching or enhancing of the luminescence intensity resulting from the specific analyte–nanocrystal interactions. Although these nanocrystal suspensions exhibit outstanding biosensing ability, the issue of suspension stability prevents them from being suitable for sensing device assembly. On the other hand, nanowire arrays of fluorescent semiconductors, such as CdS, may serve as a better format for sensing device assembly.

CdS is one of the most important II–VI semiconductors due to its vital optoelectronic applications in lasers,[8] photonic circuit elements,[9] and field emission.[10] In addition, the interactions between CdS nanocrystals and biomolecules such as amino acids[11] and DNA[12] have been discussed in response to the needs of biocompatibility when incorporating inorganic materials into living cells. For example, CdS nanoparticles that are surface-modified by peptides have been used to detect copper and silver ions.[13] These nanoparticles can possibly be further incorporated into living cells to monitor the concentrations of metal ions.

Tyrosine and serine, both amino acids with uncharged polar R groups, serve as the model system for the present differential sensing approach. These two amino acids possess the same functional groups, namely amino, carboxylic, and hydroxyl, and consequently it is difficult to differentiate them. Herein, a successful photoluminescence-based approach for this purpose is described. Suitable amounts of powdered amino acid were dissolved in a phosphate (PBS) buffer or a NaOH/KCl solution at desired pH values for preparation of amino acid solutions of different concentrations. CdS nanowire arrays were fabricated via a non-catalytic, template-free metal-organic vapor deposition (MOCVD) process. The detailed synthetic procedures for the nanowire arrays have been described by us earlier[10] and are briefly described in the Experimental Section.

When the amino acid solution is in contact with the nanowire arrays, the photoluminescence (PL) intensity of the nanowire arrays is affected through interactions between the nanowires and the amino acid molecules. The effect may be positive or negative, depending on the detailed molecular structure assumed by the amino acid molecules at specific pH values. Protonated $-NH_2$ groups ($-NH_3^+$) formed at low pH act as scavengers of the excited electrons of the photon-absorption-induced electron–hole pairs and thus suppress the PL of the nanowire arrays, whereas dissociated $-OH$ groups ($-O^-$) formed at high pH serve as the passivation species for the surface trap states of the nanowires to enhance the PL performance.[7] Tyrosine possesses a phenolic $-OH$, whereas serine possesses an alkyl $-OH$, which dissociates at a higher pH. Differential sensing of the two amino acids can thus be achieved by monitoring the PL behavior at suitable pHs. Note that the three pK values (pK_1, pK_2, and pK_R) of the two amino acids are quite close, except for pK_R, (2.20, 9.11, and 10.13 for tyrosine vs 2.19, 9.21, and 13 for serine).[14,15] In light of this information, one could set the differential pH according to the pK_2 (α-NH_3^+) and pK_R (R group) of the two amino acids. The difference in the two pK_R values leaves enough scope for the differential sensing of the two amino acids. At low pH, the amino acid solutions possess enough protonated $-NH_2$ to scavenge the excited electrons, thus reducing the PL intensity of the nanowire

[a] *Dr. Y.-F. Lin, W.-Y. Cheng, Dr. S.-Y. Lu*
Department of Chemical Engineering
National Tsing-Hua University
Hsinchu 30013 (Taiwan, R.O.C.)
Fax: (+886) 3-571-5408
E-mail: sylu@mx.nthu.edu.tw

[b] *Dr. Y.-J. Hsu*
Department of Materials Science and Engineering
National Chiao-Tung University
Hsinchu 30010 (Taiwan, R.O.C.)

arrays. As the pH of the solution increases, deprotonation of $-NH_3^+$ takes place and the dissociation of the –OH groups becomes significant, turning the role of the amino acid from electron scavenger to passivation reagent and consequently enhancing the PL intensity of the nanowire arrays.

Herein, PL spectra of the nanowire arrays were obtained for tyrosine solutions of different concentrations at pH 7 and 11, whereas those for serine solutions were obtained at pH 11 and 13. One would expect the PL spectra of the analytes (tyrosine and serine) collected at the lower pH values to decrease in intensity with increasing analyte concentration, whereas those acquired at the higher pHs should show an enhancement in intensity with increasing analyte concentration. The contrasting trend in PL intensity expected at pH 11 for the tyrosine and serine solutions then serves as a checkpoint for this differential sensing approach.

2. Results and Discussion

The morphology of the nanowire array samples was first investigated with SEM. In Figure 1b, well-aligned CdS nanowire arrays, accompanied by a buffer layer of about 1 μm thick on the silicon substrate surface are shown. The XRD pattern of the as-prepared CdS nanowire arrays is shown in Figure 1a, together with the XRD pattern of the reference wurtzite CdS crystals (JCPDS file no. 06-0314) for comparison. The as-grown CdS nanowire arrays can be indexed with wurtzite crystal structures. The diffraction peak of (0002) is much more pronounced than in the reference powder samples, which implies that the as-prepared CdS samples were grown in the preferential direction of [0001].

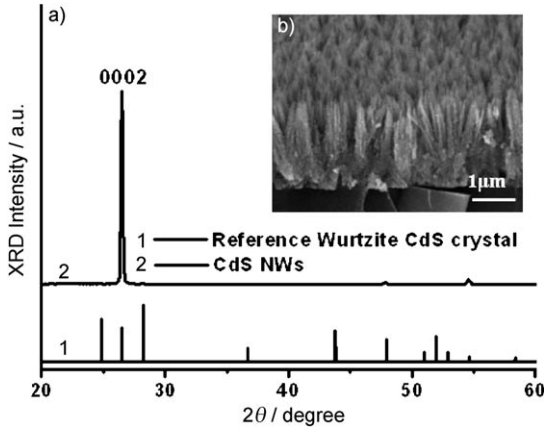

Figure 1. a) XRD pattern and b) SEM image of the CdS nanowire arrays.

The detailed crystal structure of the CdS nanowires was further characterized with a transmission electron microscope (TEM) and a high-resolution transmission microscope (HRTEM), as shown in Figure 2. The dot selected-area electron diffraction (SAED) pattern suggests single crystallinity for the CdS nanowires, and the lattice-resolved TEM image shows that the CdS nanowires grow along the [0001] direction, as shown in Figure 2c.

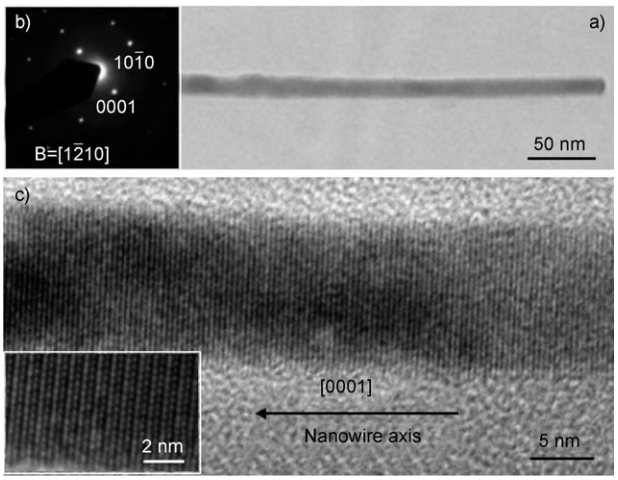

Figure 2. a) Low-magnification TEM image, b) corresponding SAED pattern, c) high-resolution TEM images of the CdS nanowires.

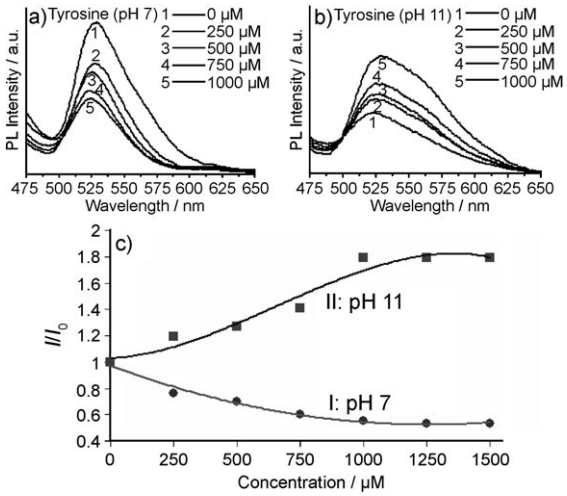

Figure 3. PL spectra of CdS nanowire arrays toward tyrosine sensing at different tyrosine concentrations at a) pH 7 and b) pH 11. c) Plot of I/I_0 vs tyrosine concentration at pH 7 (I) and pH 11 (II). The excitation wavelength is 380 nm.

Figure 3a compares the PL spectra of the CdS nanowire arrays when exposed to tyrosine solutions of different concentrations at pH 7. Two points stand out. First, as expected, the PL intensity drops with increasing tyrosine concentration. Second, the extent of depression does not correlate linearly with the tyrosine concentration, implying a mix of static and dynamic quenchings. In Figure 3c, I/I_0 vs the tyrosine concentration is plotted, where I_0 and I are the PL intensities in the absence and presence of tyrosine, respectively. The non-linearity of the curves is evident from Figure 3c, implying that this quenching/enhancing process does not follow the conventional Stern–Volmer model.[16] In fact, the feature of the curves signifies the existence of both static and dynamic quenchings/enhancement for this system.[16] This phenomenon is different

from that observed for the quenching/enhancing process encountered in nanocrystal suspensions, for which only static quenching is observed and the Stern–Volmer model is obeyed.[4,5,11]

In fact, quenching/enhancing phenomena involve a process called diffuse-and-incorporate, commonly encountered in nature and in industrial processes, such as heterogeneous catalysis, ligand–receptor binding, crystal growth and the capture of aerosol pollutants, to name but a few.[17] This process involves diffusion of small entities toward much larger and relatively immobile inclusions, and subsequent incorporation of these small entities onto the inclusions. For such processes, the overall rate is a combination of the individual rates of the two sub-processes, diffusion and surface incorporation.[18] At extreme scenarios, one of the two sub-processes can be neglected. For example, for processes limited by surface incorporation, the diffusion sub-process proceeds much faster than the surface incorporation sub-process. Consequently, surface incorporation becomes the bottleneck of the whole process and the overall rate is dominated by its rate. The quenching (or enhancing) phenomenon that occurs in nanocrystal suspensions involves such an extreme scenario in which the analyte diffusion to the nanocrystal surface encounters no particular resistance, as the suspended nanocrystals can readily be accessed by the surrounding analyte molecules. Under these circumstances, the analyte concentration at the nanocrystal surface, which determines the extent of quenching or enhancing, is directly proportional to the analyte concentration in the bulk, and thus the quenching (or enhancing) effect is directly proportional to the analyte concentration in the bulk. Consequently, a linear relationship results between the extent of quenching (or enhancing) and the analyte concentration, a typical static quenching phenomenon.

For this system, tyrosine molecules have to diffuse into the nanowire arrays to reach the nanowire surfaces for quenching (or enhancing) to occur. However, as the nanowire arrays are densely distributed, they present a large mass transfer resistance to the analyte diffusion. As a result, the analyte diffusion sub-process plays at least a comparable role to the analyte surface incorporation sub-process in determining the overall rate and the I/I_0 vs analyte concentration curves become non-linear for the quenching or enhancing process. Consequently, a dynamic character is introduced to the basic static quenching (or enhancing) process.

The distinct PL behavior of the CdS nanowire arrays toward tyrosine solutions of different concentrations at pH 11 is shown in Figure 3b. At this pH, the PL intensity of the CdS nanowire arrays increases with increasing tyrosine concentration, instead of decreases as it does at a pH of 7. The relation between the intensity enhancement and tyrosine concentration is non-linear as shown in curve II of Figure 3c, indicating the co-existence of static and dynamic passivation.

We now turn to the sensing of serine by the CdS nanowire arrays. Figure 4a shows the PL spectra of the CdS nanowire arrays when exposed to serine solutions of pH 11 at different serine concentrations. The corresponding results for serine solutions conducted at pH 13 are presented in Figure 4b for comparison. Evidently, the PL of the two amino acids at the two chosen pHs stand in contrast to each other, with the intensity quenched at pH 11 and enhanced at pH 13. In both instances, the intensity ratio correlates non-linearly with the analyte concentration, as shown in curves I and II of Figure 4c, characteristic of the presence of both static and dynamic interaction events, quenching or passivation.

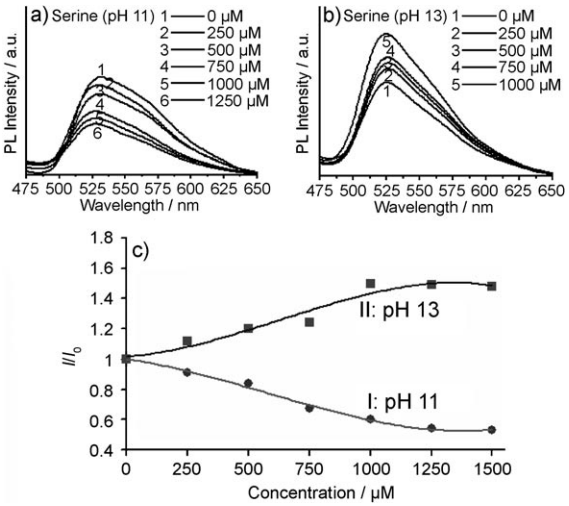

Figure 4. PL spectra of CdS nanowire arrays toward serine sensing at different serine concentrations at a) pH 11 and b) pH 13. c) Plot of I/I_0 vs serine concentration at pH 11 (I) and pH 13 (II). The excitation wavelength is 380 nm.

The contrasting PL behavior of the CdS nanowire arrays with increasing analyte concentration conducted at two distinct pH values is the same for tyrosine and serine, except that the specific pH values at which the opposite trend occurs are different for the two amino acid solutions. Thus by comparing the PL trends at a suitable pH value for the two amino acid solutions, one can differentiate between them. Herein, a pH of 11 was chosen to reveal the difference between tyrosine and serine in their effects on the PL intensity of the nanowire arrays. At pH 11, tyrosine solutions enhance, whereas serine solutions suppress, the PL intensity of the nanowire arrays, as is evident from the comparison of curves I and II of Figure 5, from which their differentiation can be concluded.

The proposed mechanisms of quenching and enhancement processes at different pH value are illustrated in Figure 6. In Figure 6a, the protonated $-NH_2$ groups ($-NH_3^+$) that form at

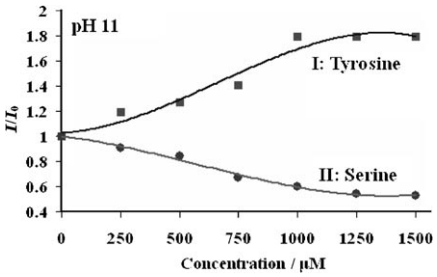

Figure 5. Plots of I/I_0 vs tyrosine (I) and serine (II) concentrations at pH 11.

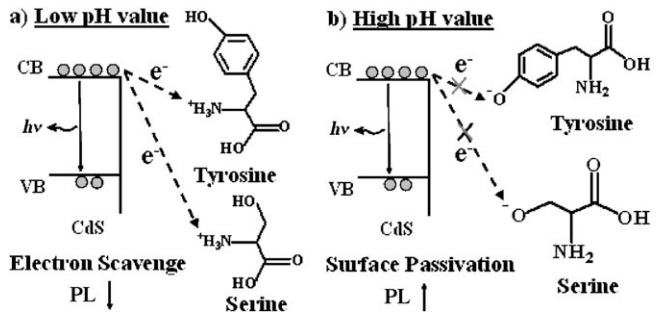

Figure 6. Proposed mechanism of quenching and enhancement processes at a) low and b) high pHs.

low pH act as scavengers of the excited electrons located in the conduction band of the photon-absorption-induced electron–hole pairs and thus suppress the PL of the nanowire arrays. On the other hand, dissociated –OH groups, $-O^-$, formed at high pH, repel the electrons located in the conduction band and thus prevent electron transfer to enable the passivation of the surface trap states of the nanowires, which should enhance the PL performance,[7] as illustrated in Figure 6b. This development can readily be extended to other amino acid pairs of less structural similarity than the pair presented herein for differential sensing purposes. However, the application of these procedures to mixtures of amino acids requires further study.

3. Conclusions

We have successfully demonstrated the differential sensing of tyrosine and serine with well-aligned CdS nanowire arrays by exploring the pH-dependent PL behavior of the nanowire arrays toward exposure to the two amino acid solutions. This development is much better suited for further sensing device assembly than nanocrystal suspension systems, and can also be extended to differential sensing of other biological substances.

Experimental Section

CdS nanowire arrays were grown on Si substrates via a non-catalytic and template-free MOCVD process using the single-source precursor $Cd[S_2CN(C_3H_7)_2]_2$.[10] The furnace temperature was set at 450 °C and the deposits were collected on Si substrates. All depositions were run for 6 hr with a carrier gas flow rate of 50 sccm (standard cubic centimetres per minute) and a system pressure of 30 torr.

The sensing of the amino acids was conducted with a photoluminescence spectrometer, a Hitachi F-4500 equipped with a xenon lamp (150 W) and a 700 V photomultiplier tube as the detector. The excitation wavelength was set at 380 nm. The CdS nanowire arrays, grown on Si substrates, were immersed in a tyrosine or serine solution of desired pH and concentration. This sample cell was then mounted on the sample holder of the spectrometer for the PL measurements.

Acknowledgements

The authors gratefully acknowledge the support of the National Science Council of the Republic of China (Taiwan) under grant NSC-96-2628-E-007-015-MY2.

Keywords: amino acids · CdS · differential sensing · nanostructures · photophysics

[1] M. Bruchez, Jr., M. M. Moronne, P. G. S. Weiss, A. P. Alivisatos, *Science* **1998**, *281*, 2013.
[2] W. C. W. Chan, S. Nie, *Science* **1998**, *281*, 2016.
[3] a) X. Ji, J. Zheng, J. Xu, V. K. Rastogi, T.-C. Cheng, J. J. DeFrank, R. M. Leblanc, *J. Phys. Chem. B* **2005**, *109*, 3793; b) C. A. Constantine, K. M. Gattas-Asfura, S. V. Mello, G. Crespo, V. Rastogi, T.-C. Cheng, J. J. DeFrank, R. M. Leblanc, *J. Phys. Chem. B* **2003**, *107*, 13762; c) C. A. Constantine, K. M. Gattas-Asfura, S. V. Mello, G. Crespo, V. Rastogi, T.-C. Cheng, J. J. DeFrank, R. M. Leblanc, *Langmuir* **2003**, *19*, 9863.
[4] J. Liang, S. Huang, D. Zeng, Z. He, X. Ji, X. Ai, H. Yang, *Talanta* **2006**, *69*, 126.
[5] E. Chang, J. S. Miller, J. Sun, W. W. Yu, V. L. Colvin, R. Drezek, J. L. West, *Biochem. Biophys. Res. Commun.* **2005**, *334*, 1317.
[6] C.-P. Huang, Y.-K. Li, T.-M. Chen, *Biosens. Bioelectron.* **2007**, *22*, 1835.
[7] A. Priyam, A. Chatterjee, S. K. Das, A. Saha, *Chem. Commun.* **2005**, 4122.
[8] R. Agarwal, C. J. Barrelet, C. M. Lieber, *Nano Lett.* **2005**, *5*, 917.
[9] C. J. Barrelet, A. B. Greytak, C. M. Lieber, *Nano Lett.* **2004**, *4*, 1981.
[10] a) Y.-F. Lin, Y.-J. Hsu, S.-Y. Lu, S.-C. Kung, *Chem. Commun.* **2006**, 2391; b) Y.-F. Lin, Y.-J. Hsu, S.-Y. Lu, K.-T. Chen, T.-Y. Tseng, *J. Phys. Chem. C* **2007**, *111*, 13418; c) Q. T. Chen, T. Li, A. Zhao, Y. Qian, D. Yu, W. Yu, *Chem. Lett.* **2004**, *33*, 1088.
[11] a) A. Chatterjee, A. Priyam, S. K. Das, A. Saha, *J. Colloid Interface Sci.* **2006**, *294*, 334; b) A. Datta, A. Saha, A. K. Sinha, S. N. Bhattacharyya, S. Chatterjee, *J. Photochem. Photobiol. B* **2005**, *78*, 69.
[12] a) S. K. Kulkarni, A. S. Ethiraj, S. Kharrazi, D. N. Deobagkar, D. D. Deobagkar, *Biosens. Bioelectron.* **2005**, *21*, 95; b) T. Torimoto, M. Yamashita, S. Kuwabata, T. S akata, H. Mori, H. Yoneyama, *J. Phys. Chem. B* **1999**, *103*, 8799.
[13] K. M. Gattás-Asfura, R. M. Leblanc, *Chem. Commun.* **2003**, 2684.
[14] R. K. Murray, D. K. Granner, P. A. Mayes, V. W. Rodwell, *Harper's Biochemistry*, Appleton and Lange, Stamford, **2000**, p. 29.
[15] G. L. Zubay, W. W. Parson, D. E. Vance, *Principle of Biochemistry*, Wm. C. Brown, Dubuque, **1995**, p. 54.
[16] a) J. R. Lakowicz, *Principles of Fluorescence Spectroscopy*, Plenum, New York, **1983**, chap. 9, p. 257; b) W. J. Jin, J. M. Costa-Fernandez, R. Pereiro, A. Sanz-Medel, *Anal. Chim. Acta* **2004**, *522*, 1.
[17] E. V. Albano, *Heterog. Chem. Rev.* **1996**, *3*, 389.
[18] a) S.-Y. Lu, Y.-M. Yen, *J. Chem. Phys.* **2002**, *116*, 3128; b) S.-Y. Lu, Y.-M. Yen, C.-Y. Tseng, H.-K. Tsao, *J. Chem. Phys.* **2002**, *117*, 3431; c) S.-Y. Lu, *J. Chem. Phys.* **2004**, *120*, 3997.

Received: October 6, 2008
Published online on February 2, 2009

